**Supplementary Information**

# Shape-programable magneto-active elastomers composites for curve and biomimetic behavior imitation

Di Gong, Fan Yang*, Dezhao Lin, Wenbo Qian, Ruihong Li, Chenghong Li, Hongwei Chen and Sheng Jia

*Research Center for Intelligent Materials and Structures (CIMS), College of Mechanical Engineering and Automation, Huaqiao University, Xiamen, Fujian, P.R.China*

** Corresponding author: xmyf@hotmail.com (F. Yang).*

In this Supplementary Document, the equilibrium orientation of the soft-magnetic particles based MAEs elements under applied magnetic fields will be investigated.

## S1. Analysis of equilibrium orientation of the MAEs elements.

By applying magnetic field during the curing process, the carbonyl iron powders (CIPs) in MAEs will be arranged along the direction of applied curing magnetic fields, and then generated chain-like structures.[1-5] After the curing procedure, under the condition that applying a external magnetic field, the iron particles will be magnetized and interact with each other and generate a magnetic torque to rotate the MAEs. Here, it should be noted that in this study the MAEs elements will be treated as the rigid body as the main function of this kind of MAEs is to drive the composite to generate the required curves. After turning off the magnetic field, the iron particles will be demagnetized, no magnetic torque applied under this condition.

To illustrate the driving properties of the MAEs materials, the simple analysis based on the assumption of well-defined chains in the MAEs materials, which is widely utilized to reflect the tendency of the particle arrangement in MAEs materials,[6,7] has been presented in Fig. S1a. It has been shown that this simple methodology can predict the rotation of the MAEs elements with different chain angles and the behavior of the presented shape-programmable MAEs material with good accuracy. It should be noted that in practical situations the chains in MAEs materials will not be well defined, [8-13] and detailed analysis of its driving properties of this kind of MAEs, which include the deformation, extension, surface effects, and other properties, is definitely required for the better application of this kind of materials.

Under the applied magnetic fields, the magnetic moment ($m_p$) of each CIPs particle in MAEs can be expressed as:[13]

$$m_p = \chi_m V H \#(S1)$$

where $\chi_m$, $V$ and $H$ are the magnetic susceptibility and volume of the CIPs particles, and the applied magnetic field intensity, respectively. There are two magnetic torque applying to the MAEs element under the applied magnetic fields, as shown in Fig. S1a: (1) the torque induced by the adjacent particles in chains ($T_p$); (2) the torque induced by the adjacent particles between chains ($T_c$), as shown in Fig. S1a. Here, it should be noted that for the seeking of clear expression, in this study (1) the magnetic moment of each CIPs particle is assumed to be with the same direction as the direction of the applied external magnetic field, and then the interactions between the applied

magnetic field ($B$) and the magnetic moment ($m_p$) of each CIPs particle can be ignored;[6,7,14] (2) the torques generated by the elastic force and the gravity have been ignored. Considering the above, the total torque ($T_m$) applying to the MAEs element under the applied magnetic field can be expressed as:[6,7,14]

$$T_m = T_p - T_c = \frac{3\mu_0 n m_p^{\ 2}}{2\pi}\left(\frac{\sin 2\alpha}{d^3} - \frac{\sin 2\theta}{D^3}\right) \#(S2)$$

where parameters $\mu_0$ and $n$ represent the permeability of vacuum and the number of CIPs particles. Parameters $\alpha$ and $\theta$ represent angles between the chain-like structure and the direction of applied external magnetic field, and between the neural line of the MAEs element and the direction of applied external magnetic field, as shown in Fig. S1a. Parameters $d$ and $D$ represent the distance between adjacent particles in chains and between adjacent chains respectively, as shown in Fig. S1a.

Based on Equation (S2), it can be found that in theory the MAEs element will reach its equilibrium orientation under the condition of $T_m = 0$.

**S2. Test of equilibrium orientations of the MAEs elements.**

7 MAEs elements (Sample A to F) with different chain angles ($\theta_c$), as summarized in Table 2, were cut into square shape with the same size, as shown in Fig. 1d. Applying the vertical magnetic fields gradually, as shown in Fig. S1b, the MAEs elements, which were placed horizontally on an acrylic panel, will rotate around the boundary, as shown in Fig. S1c, with the increase of the applied

magnetic field, until it reaches the final equilibrium orientation (around 150 mT in this study), which will not be changed with the increase of the magnetic field anymore. The orientation angles ($\theta_A$) of MAEs elements with different chain angles ($\theta_c$) were recorded and the results have been summarized in Fig. S1d (diagonal lines hatch). To investigate the effect of the gravity, the orientation angles ($\theta_A$) of MAEs elements with suspending boundary have also been recorded and the results have been presented in Fig. S1d (reticular hatch), from which one can easily find that the effect of gravity (the maximum deviation is less than 1%) to the orientation angles ($\theta_A$) can be ignored for this kind of small size MAEs samples. Therefore, the orientation angles ($\theta_A$) for the MAEs samples with free placed boundary, as summarized in Table 2, will be utilized to fabricate the MAEs composites.

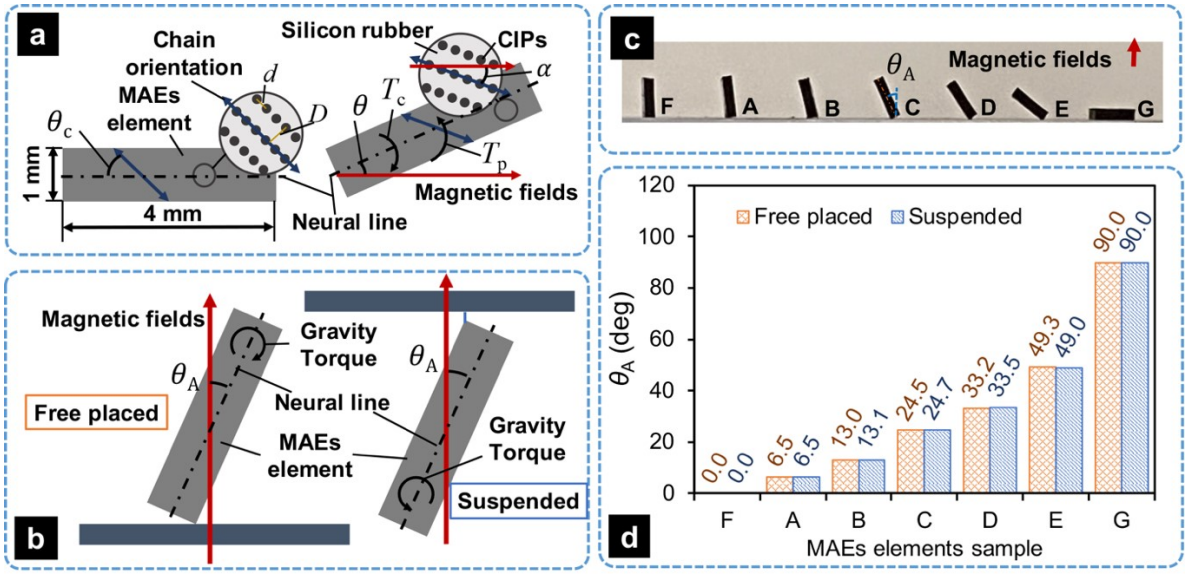


**Fig. S1** The rotation of the MAEs elements. (a) The schematic of a MAEs element under applied magnetic field. (b) The static equilibrium position of the MAEs element under suspended and freely placed conditions. (c) The equilibrium orientation (test result) of the MAEs elements. (d) The angle

between applied magnetic field and the neural line of the MAEs elements under freely placed and suspended conditions.

## References


[1] A. Goshkoderia, V. Chen, J. Li, A. Juhl, P. Buskohl and S. Rudykh, *Phys. Rev. Lett.*, 2020, **124**, 158002.

[2] J. Carlson and M. Jolly, *Mechatronics*, 2000, **10**, 555-569.

[3] D. Günther, D. Borin, S. Günther and S. Odenbach, *Smart Mater. Struc.*, 2012, **21**, 015005.

[4] T. Borbath, S. Günther, D. Borin, T. Gündermann and S. Odenbach, *Smart Mater. Struc.*, 2012, **21**, 105018.

[5] P. Sánchez, E.Minina, S. Kantorovich and E. Kramarenko, Soft Matter, 2019, **15**, 175–189.

[6] R. Erb, J, Martin, R. Soheilian, C. Pan and J. Barber, *Adv. Funct. Mater.*, 2016, **26**, 3859-3880.

[7] J. Kim, S. Chung, S.-E., Choi, H. Lee, J. Kim and S. Kwon, *Nat. Mater.*, 2011, **10**, 747-752.

[8] A. Snarskii, M. Shamonin and P. Yuskevich, *J. Magn. Magn. Mater.*, 2021, **517**, 167392.

[9] A. Snarskii, M. Shamonin, P. Yuskevich, D. Saveliev and I. Belyaeva, *Physica A*, 2020, **560**, 125170.

[10] G. Stepanov, D. Borin, A. Bakhtiiarov, D. Loabanov and P. Storozhenko, *Smart Mater. Struc.*, 2021, **30**, 015023.

[11] M. Cantera, M. Behrooz, R. Gibson and F. Gordaninejad, *Smart Mater. Struc.*, 2017, **26**, 023001.

[12] M. Lallart, G. Sebald, F. Diguet, J. Cavaille and M. Nakano, *J. Appl. Phys.*, 2017, **122**, 103902.

[13] G. Pessot, R. Weeber, C. Holm, H. Löwen and A. Menzel, *J. Phys. Condens. Matter*, 2015, **27**, 325105.

[14] D. Griffiths, *Introduction to Electrodynamics*, Prentice Hall, Upper Saddle River, NJ, 2005.